Corrosion Resistance of Ultrafine-grained Titanium Alloys in Different Corrosive Environments

Yuecheng Dong[a,b,c,*], Xin Li[a,d], Zequn Yu[a], Igor Alexandrov[e], Hui Chang[a], Lian Zhou[a]

[a] College of Materials Science and Engineering and Tech Institute for Advanced Materials, Nanjing Tech University, Nanjing, 211816, China

[b] State Key Laboratory of Metal Material for Marine Equipment and Application, Anshan, 114000, China

[c] Naval Research Institute, Beijing, 100000, China

[d] Jiangsu Collaborative Innovation Center for Advanced Inorganic Function Composites, Nanjing Tech University, Nanjing, 211816, China

[e] Department of Physics, Ufa State Aviation Technical University, Ufa, 450000, Russia

* dongyuecheng@njtech.edu.cn

Abstract

Corrosion Resistance of ultrafine-grained (UFG) titanium alloys fabricated by equal channel angular pressing (ECAP) was investigated in this study. Electrochemical measurements of pure Ti and Ti-6Al-7Nb alloy were conducted in 3.5 wt.% NaCl and Ringer's solution separately. Results indicated that both ultrafine-grained pure Ti and Ti-6Al-7Nb alloy had much lower corrosion current density than annealed coarse-grained counterparts in the specified corrosive environment.

1. Introduction

Titanium alloy is widely applied in the field of chemical engineering, biomedical and marine industries due to high specific strength and corrosion resistance[1-3]. Ultrafine-grained (UFG) and nanocrystalline (NC) materials with high strength and ductility processed by severe plastic deformation are widely studied in the recent decades[4-6]. Compared with large number researches on mechanical behavior of nanocrystalline materials, corrosion resistance is rarely studied and results indicated inconsistent, even within the same alloy system[7,8].

Nie[9] et al. investigated corrosion behavior of UFG-Ti processed by HPT in 3.5 wt.% NaCl solution, which found coarse grain (CG) Ti possess better corrosion resistance than UFG Ti. Garbacz[10] studied corrosion behavior of UFG-Ti fabricated by hydrostatic extrusion (HE) by Auger electron spectroscopy (AES) and Ar^+ sputtering technology in 0.15 mol/L NaCl solution, results shown that corrosion resistance decrease for UFG-Ti and thickness of passive film formed on the surface was no much more different. However, Balyanov[11] founded that UFG-Ti processed by ECAP possess better corrosion resistance than CG-Ti in the HCl and H_2SO_4 solutions, which could be attributed to the rapid formation of passive film for UFG-Ti. Fattah-Alhosseini[12,13] fabricated UFG-Ti by the method of friction stir processed (FSP) and accumulative roll bonding (ARB), results indicated that corrosion current and passive current density decreased with decreasing grain size and corrosion potential increased, which revealed that corrosion resistance of UFG-Ti is better than CG-Ti, the same conclusion was also founded in researches of Gurao[14] and Raducanu[15], who studied corrosion behavior of UFG-Ti and UFG-Ti-10Zr-5Nb-5Ta in simulated body fluid separately.

Obviously, different corrosive environment and UFG microstructure by various process methods could be responsible for inconsistent conclusion. In the present work, corrosion behavior of UFG-Ti and UFG-Ti-6Al-7Nb processed by ECAP was investigated in 3.5 wt.% NaCl and Ringer's solution respectively. The aim of our studies is trying to clarify the effect of grain size on corrosion behavior.

2. Experimental

Commercial purity Ti Grade 4 (CP Ti) and Ti-6Al-7Nb alloy were used in the present study, ECAP was conducted in Ufa State Aviation Technical University. Chemical composition is listed in Table 1 and Table 2.

Table 1. Chemical composition of CP Ti Grade 4

Element	Ti	Fe	C	H	N	O	Others
wt%	Balance	0.50	0.08	0.0125	0.05	0.40	0.40

Table 2. Chemical composition of Ti-6Al-7Nb alloy

Element	Ti	Nb	Al	Fe	V	C	O	N	Others
wt%	Balance	6.94	6.06	0.15	＜0.05	0.01	0.17	0.0027	＜0.05

Microstructure characterization of samples was performed by the method of electron backscattered diffraction (EBSD). Before performing the EBSD investigation, the samples were mechanically polished with abrasive paper and polishing paste, then subjected to electro-polishing (solution: $HClO_4$: C_2H_5OH =19:1 (volume ratio); voltage: 40V; polishing time: 90s). Automated EBSD scans were using Flamenco data acquisition software. All the data were processed with HKL Technology Channel 5 software.

Corrosion behavior of samples was investigated by potentiodynamic polarization. electrochemical test was performed using CHI660E electrochemical station in 3.5 wt% NaCl solution for CG-Ti, potentiodynamic polarization data were acquired at a sweep rate of 2 mV/s from -250 mV to 800 mV/SCE. On the other hand, electrochemical test was performed using CHI660E electrochemical station in Ringer's solution for Ti-6Al-7Nb, potentiodynamic polarization data were acquired at a sweep rate of 2 mV/s from -800 mV to 800 mV/SCE. The electrolyte was a naturally aerated Ringer's solution (an aqueous solution of the chlorides of sodium, potassium, and calcium that is isotonic to animal tissue and is used topically as a physiological saline), of which composition is 9g NaCl, 0.42 g KCl and 0.25 g $CaCl_2$. The open circuit potential variation with time was measured in Ringer's solution at 37℃,the pH is adjusted to 7.

3. Results and Discussion

Microstructure of the CG-Ti and Ti-6Al-7Nb is illustrated in Figure 1 and Figure 2, It can be seen fairly equiaxed and homogeneous grains were consisted in the microstructure, the grain size distribution calculated by Technology Channel 5 software indicates that the average grain size of CG-Ti is 142.9μm and large volume fraction concentrates (∼8.5%) on the grain size interval 50~60μm (Figure 1b), at the same time, average grain size of the Ti-6Al-7Nb is 13.8μm and large volume fraction concentrates (∼45%) on the grain size interval 5~10μm (Figure 2b).

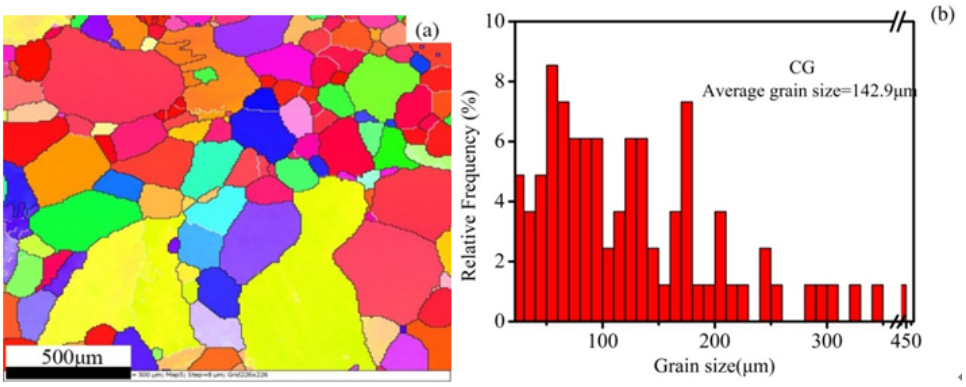

Fig 1. EBSD results of microstructure (a) and grain size distribution (b) of CG Ti

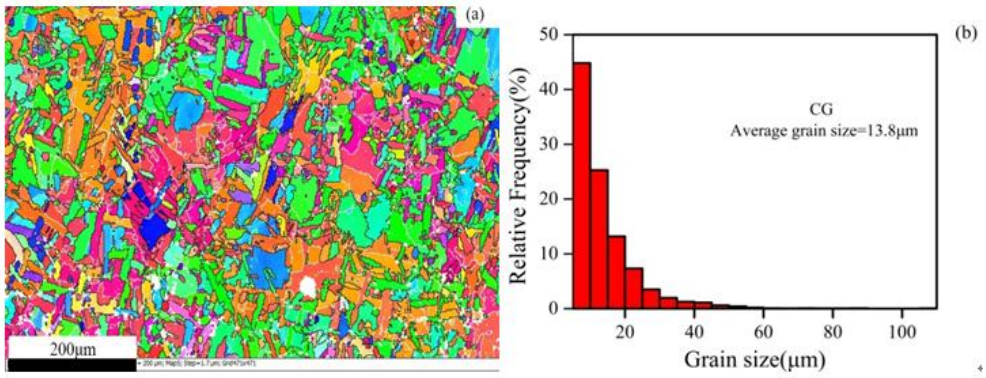

Fig 2. EBSD results of microstructure (a) and grain size distribution (b) of CG Ti-6Al-7Nb

Microstructure of the UFG-Ti and UFG-Ti-6Al-7Nb processed by ECAP is illustrated in Figure 3 and Figure 4, which displays a remarkable grain refinement resulted from the large volume of plastic deformation applied during ECAP process. Microstructure of UFG-Ti and UFG-Ti-6Al-7Nb sample also reveals equiaxed and homogeneous grains, the grain size distribution calculated by Technology Channel 5 software indicates that the average grain size of Ti reduced to 0.567μm and large volume fraction concentrates (∼20%) on the grain size interval 300~400 nm (Figure 3b), at the same time, average grain size of the UHG-Ti-6Al-7Nb reduced to 0.4μm and large volume fraction concentrates (∼55%) on the grain size interval 200-400nm (Figure 4b).

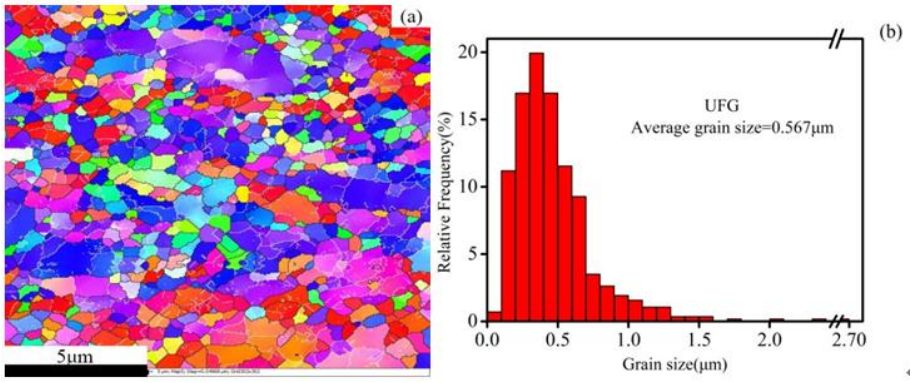

Fig 3. EBSD results of microstructure (a) and grain size distribution (b) of UFG Ti

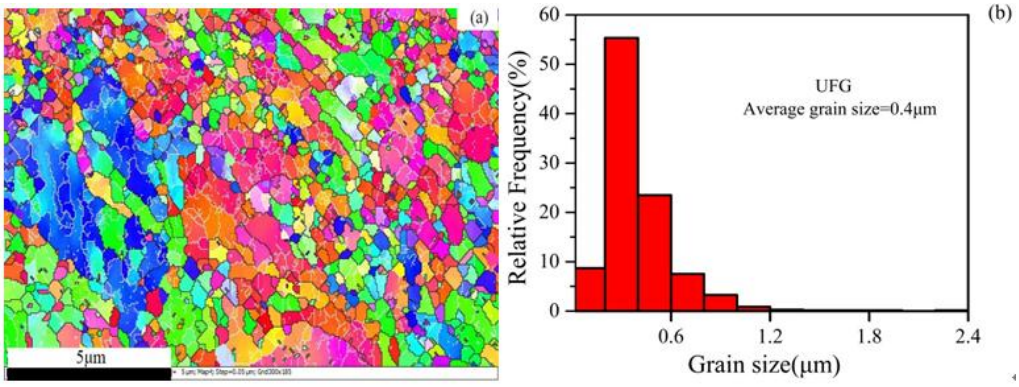

Fig 4. EBSD results of microstructure (a) and grain size distribution (b) of UFG Ti-6Al-7Nb

3.2 Corrosion behavior

Potentiodynamic polarization curves of CG-Ti and UFG-Ti processed by ECAP in 3.5 wt.% NaCl solution is illustrated in Fig.5. The results show that both CG-Ti and UFG-Ti have similar polarization behaviors，all samples exhibited obvious pitting corrosion phenomenon, potential from -0.276 V to 0.091 V is passivation region for CG-Ti, passivation range is about 0.367V, pitting corrosion happened when the potential reached to 0.091 V. On the other hand, the passivation range of UFG-Ti is 0.315 V, passive film cracked when the potential reached to 0.117 V. The major reaction of the Tafel cathodic regions is $O_2+4H^++4e^- = 2H_2O$, while the major reaction of the Tafel anodic regions is $Ti\text{-}4e^- = Ti^{4+}$. The mean corrosion potential (E_{corr}) and corrosion current density (I_{corr}) values obtained from all the tested polarization curves are listed in Table 3. The E_{corr} and I_{corr} values were determined by extrapolating the linear Tafel segments of the anode and cathode polarization curves. According to Table 3, the I_{corr} of initial CG-Ti is 4.8 times higher than UFG-Ti processed by ECAP, from which can be concluded that the corrosion resistance of UFG-Ti is superior to the CG-Ti.

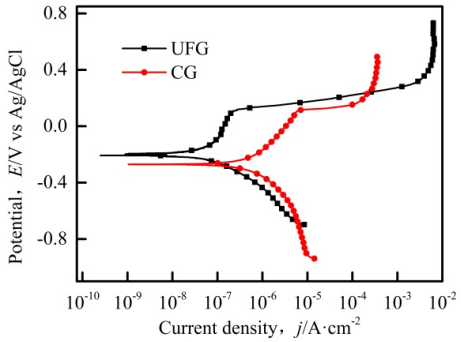

Fig 5. Potentiodynamic polarization curves of samples in 3.5 wt.% NaCl solution

Table 3.Corrosion Potential and corrosion current density of Ti in 3.5 wt.% NaCl Solution

Sample	CG	UFG
E_{corr} (mV)	-276	-198
I_{corr} (μA/cm^2)	0.394	0.0815

Potentiodynamic polarization curves of CG-Ti-6Al-7Nb and UFG-Ti-6Al-7Nb processed by ECAP in Ringer's solution is illustrated in Fig.6. All of the samples exhibited the similar polarization behavior and reached their respective stable passive current densities as the potential increased. Potential from -0.228 V to 0.191 V is passivation region for CG-Ti-6Al-7Nb, passivation range is about 0.419V, pitting corrosion happened when the potential reached to 0.191 V. On the other hand, passivation range increased to 0.478 V for UFG-Ti-6Al-7Nb, much higher than CG one, passive film cracked when the potential reached to 0.230 V. The mean corrosion potential and corrosion current density values obtained from all the tested polarization curves are listed in Table 4. Results indicated that corrosion current density of CG-Ti-6Al-7Nb is also higher than the UFG-Ti-6Al-7Nb, which means that the corrosion resistance of UFG-Ti-6Al-7Nb is better than CG-Ti-6Al-7Nb.

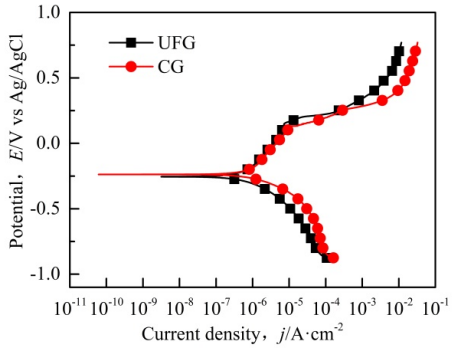

Fig 6. Potentiodynamic polarization curves of tested samples in Ringer's solution

Table 4.Corrosion Potential and Corrosion Current density of Ti-6Al-7Nb in Ringer's Solution

Sample	CG	UFG
E_{corr} (mV)	-228	-248
I_{corr} (μA/cm^2)	0.916	0.689

Titanium alloy has excellent corrosion behavior due to the formation of TiO2 passive film on the surface. However, the exhibition of high concentration of aggressive ion can penetrate passive film and reach to the interface between passive film and matrix titanium, which could form corrosive galvanic cell and make rapid reaction of matrix with aggressive ion, then lead to pitting corrosion[16]. On the other hand, pitting corrosion could be restrained due to its self-repairing ability, which means a fresh passive film could be developed to provide further protection.

Pitting corrosion is difficult to happen for UFG titanium alloy in resent research, because ECAP could introduce UFG metals with plenty of dislocation in grain interior and boundaries simultaneous, nucleation of passive film could be formed in grain interior and boundaries at the same time, which made passive film more dense and resisted penetration of aggressive ion. Sotniczuk[17] revealed that corrosion behavior improve for UFG-Ti due to slight increasing roughness of surface, which made the passive film more stable. At the same time, dramatic increase of defective promote more dense of passive film suppressed the occurrence of pitting corrosion. On the other side, passive current density of UFG Ti is much lower than CG Ti, which indicated that passivation film of UFG titanium is more prone to self-repairing after pitting corrosion. This is mainly attributed to a high storage energy in the dislocations and grain boundaries in UFG titanium alloy processed by ECAP, which is beneficial to the formation of the passivation film, thereby enhancing the self-repairing ability of the passivation film.

4. Conclusions

Corrosion behavior of ultrafine-grained Ti and Ti-6Al-7Nb fabricated by ECAP was investigated in 3.5 wt.% NaCl and Ringer's solution separetely. Electrochemical results indicated that UFG-Ti and UFG-Ti-6Al-7Nb alloy exhibits much lower corrosion current density than CG counterparts, which could be attributed to more dense and rapid self-repairing of passivation film of UFG titanium alloy.

Acknowledgements

The author acknowledges the financial assistance from the State Key Laboratory Open Source for Metal Materials and Applications for Marine Equipment (No. SKLMEA-K201807), China Postdoctoral Science Foundation (No. 2017M623392), Postgraduate Research & Practice Innovation Program of Jiangsu Province (No. SJCX19_0324), the Priority Academic Program Development of Jiangsu higher education institutions (PAPD).

References

[1] Geetha M, Singh A K, Asokamani R, et al. Progress in Materials Science. 54 (2009) 397-425.

[2] Qiao Z, Liu X Y, Zhao X C, et al. Rare Metal Materials & Engineering. 46 (2017) 2618-2622.

[3] Ralston K D, Birbilis N, Davies C H J. Scripta Materialia. 63(2010) 1201-1204.

[4] Miyamoto H. Materials Transactions. 57 (2016) 559-572.

[5] Estrin Y, Vinogradov A. International Journal of Fatigue. 32 (2010) 898-907.

[6] Rodriguez-Calvillo P, Cabrera J M. Materials Science and Engineering: A. 625 (2015) 311-320.

[7] Ravisankar B , Park J K . Transactions of the Indian Institute of Metals. 61 (2008) 51-62.

[8] Ralston K D, Birbilis N. Corrosion. 66 (2010) 075005-075005-13.

[9] Nie M, Wang C T, Qu M, et al. Journal of Materials Science. 49 (2014) 2824-2831.

[10] Garbacz H, Pisarek M, Kurzydłowski K J. Biomolecular Engineering. 24 (2007) 559-563.

[11] Balyanov A, Kutnyakova J, Amirkhanova N A, et al. Scripta Materialia. 51 (2004) 225-229.

[12] Fattah-Alhosseini A , Vakili-Azghandi M , Sheikhi M , et al. Journal of Alloys and Compounds. 704 (2017) 499-508.

[13] Fattah-Alhosseini A, Imantalab O, Ansari G. Materials Science & Engineering C. 71 (2017) 827-834.

[14] Gurao, N. P, Suwas, et al. Metallurgical & Materials Transactions A. 44 (2013) 5602-5610.

[15] Raducanu D, Vasilescu E, Cojocaru V D, et al. J Mech Behav Biomed Mater. 4 (2011) 1421-1430.

[16] Zhang B, Wang J, Wu B, et al. Nature Communications. 9 (2018) 2559.

[17] Sotniczuk A, Kuczyńska, Donata, Kubacka D, et al. Materials Science and Technology. (2017) 1-9.